The Role of Sfrp4 in Alveolar Bone and Incisor Tooth Extraction Socket Healing

The Role of *Sfrp4* in Alveolar Bone and Incisor Tooth Extraction Socket Healing

A Thesis Presented by

Muhsen Mohammad Alnasser

to

The Faculty of Medicine

In partial fulfillment of the requirements

for the degree of

Doctor of Medical Sciences

Research Mentors:

Francesca Gori, PhD

Roland Baron, DDS, PhD

Harvard School of Dental Medicine

Boston, Massachusetts

April, 2021

Dedication

I dedicate my DMSc thesis work

To my mother for her boundless love, guidance,
support, and encouragement.

To my father for his believing and faith on me.

To my wife Batool for her endless sacrifice, support, and encouragement during my educational journey.

To my daughters Reem, Mira, and new baby Maryam for bringing the happiness to my life.

To my family and friends for their care and support.

Acknowledgement

I am greatly thankful and appreciative for several people who make this research project done.

My deepest gratitude to Dr. Francesca Gori for her guidance during the journey of this Research project. Her effort was the major contributor to this research project.

I would like also to acknowledge Dr. Roland Baron for his continuous support in supervising every step in the thesis.

I would like to express my appreciation my department chair, Dr. German Gallucci, for sharing his knowledge and experience. He is the reason why I became a member of HSDM and Harvard Implantology family.

My sincere thanks to my program director, Dr. Adam Hamilton. Under his guidance and support, my dreams became true.

I would like also to express my appreciation to Dr. Dominique Rousson for his endless support and encouragement.

Special thanks to Dr. Franz Strauss and Dr. Reinhard Gruber from Department of Oral Biology, Medical University of Vienna, Austria, for sharing their experience in mice tooth extraction procedure.

Special thanks to Dorothy Zhang Hu, Dhairya Raval, Shawn Berry, all other members of Baron – Gori lab, and all members of Harvard implantology team for their guidance and support to finish this research project.

Table of Contents

Abstract

Objectives:

The purpose of this study is to explore the effects of *Sfrp4* deletion on alveolar bone and healing of incisor tooth extraction sockets.

Introduction:

There are many genetic and development bone diseases that affect the skeletal system and compromise the quality and strength of bone. Among these is Pyle's disease OMIM-265900). Pyle's disease is a disorder of bone architecture characterized by expanded trabecular metaphyses, thin cortical bone, and bone fragility. Our laboratory has linked Pyle's disease to loss of function mutations of Secreted Frizzled Receptor Protein 4 (*sFRP4*). *sFRP4* is a member of the Wnt signaling that functions as a Wnt decoy receptor and blocks all Wnt signaling cascades.

Pyle disease's patients present with abnormal cortical bone in the craniofacial skeleton, smaller heads, thin calvarium and expanded diploe, as well as dental abnormalities such as tooth decay, delayed tooth eruption, and retained deciduous teeth. However, the role of *sFRP4* deficiency in alveolar bone and tooth extraction healing is not known.

Methods:

Maxillary right incisor extractions were performed on 8 weeks (wk) old *WT* and *Sfrp4-/- (KO)* male and female mice. Mice were sacrificed one, two, and three wk after tooth extraction. Skulls were harvested for three-dimensional micro-computed tomographic (μCT) and bone histomorphometry.

Bone morphometry and 3D reconstruction were performed for both groups to explore *Sfrp4* deficiency effects on alveolar bone in maxillary incisor and molars areas. The healing socket of the extracted maxillary right incisor was analyzed by μCT, dynamic, and cellular bone histomorphometry.

Results:

Sfrp4 deletion resulted in significantly decreased bone volume and increased porosity in alveolar bone of incisor and molars areas. However, *Sfrp4* deletion did not show a significant difference in bone healing of incisor tooth socket.

Conclusion:

Similar to the phenotype seen in long bones, in alveolar bone, *Sfrp4* deletion leads to a significant decrease in cortical bone volume and increased porosity in both the incisor and molars alveolar bone areas.

Incisor socket bone healing is not affected by *Sfrp4* deletion, suggesting that simultaneous activation of canonical and non-canonical Wnt cascades by *Sfrp4* deletion does not impair socket bone healing. These findings might have direct clinical applications as patients with Pyle's disease usually presents with dental abnormalities requiring tooth extraction.

1 Introduction

1.1 Rationale of the study

There are many genetic and development bone diseases that affect the skeletal system and compromise the quality and strength of bone. Among these is Pyle's disease (OMIM-265900). Pyle's disease is a disorder of bone architecture characterized by expanded trabecular metaphyses, thin cortical bone, and bone fragility (Gorlin, Koszalka , Spranger 1970; Raad, Beighton 1987).

In collaboration with Dr. Superti-Furga's group, our laboratory has linked Pyle's disease to loss of function mutations of Secreted Frizzled Receptor Protein 4 (*sFRP4*) (Kiper, Saito, Gori et al. 2016). *sFRP4* is a member of the Wnt signaling that functions as a Wnt decoy receptor and blocks all Wnt signaling cascades (Gori, Baron 2013). Our studies have shown that *Sfrp4* deletion in mice causes skeletal deformities closely mimicking those seen in Pyle's disease and that cortical bone thinning is due to decreased periosteal apposition and increased endocortical remodeling (Figure 1) (Kiper, Saito, Gori et al. 2016). In particular, our studies have shown that cortical thinning is due to activation of non-canonical Wnt signaling (Kiper, Saito, Gori et al. 2016; Chen, Ng, Chen et al. 2019).

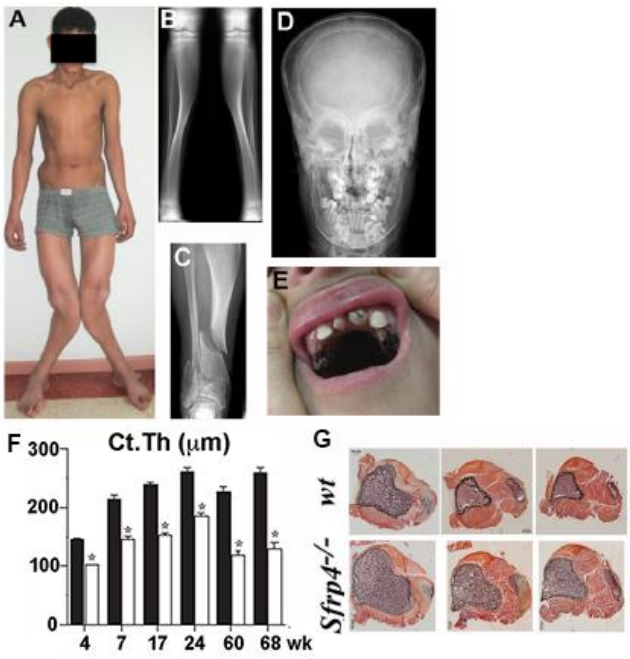

Figure 1: Skeletal deformities in Pyle disease's patients and *Sfrp4*-null mice.

A-E) Clinical and radiographic presentations in a patient diagnosed with Pyle's disease. F) microcomputed tomography (μCT) analysis of cortical thickness in femur midshaft of wild-type (black bars) and *Sfrp4*-null (open bars) mice at 4, 7, 17, 24, 60, and 68 weeks of age. G) Representative histologic features of von Kossa–stained trabecular and cortical bone in proximal tibiae of *WT* and *Sfrp4*-null mice at 4 weeks of age (Kiper, Saito, Gori et al. 2016).

Pyle's disease patients present also with abnormal bone in the craniofacial skeleton characterized by smaller heads, thin calvarium, and expanded diploe (Figure 1D). These patients present also with dental abnormalities (Figure 1E) including carious and misplaced teeth, delayed tooth eruption, and retained deciduous teeth (Kiper, Saito, Gori et al. 2016; Narayananan, Ashok, Mamatha et al. 2006). Sfrp4 is expressed in the incisor during mouse development (Leimeister, Bach, Gessle 1998), however, its role in tooth development, alveolar bone, and tooth extraction healing is not known. Tooth extraction is a routine clinical procedure that is associated with alveolar bone loss. Impaired tooth extraction socket healing negatively affects future implant treatment to replace missing teeth which leads to esthetic and functional challenges in the oral cavity. Therefore, investigating the mechanism(s) by which alveolar bone and healing of tooth extraction sockets are regulated might lead to the initial steps of developing new therapeutic approaches to favor alveolar bone healing in humans. The overall objective of this study is to explore the effects of *Sfrp4* deficiency on alveolar bone and healing of tooth extraction sockets. Our hypothesis is that *Sfrp4* influences alveolar bone homeostasis and socket healing. To test this hypothesis, we followed two independent specific aims.

1.2 Specific Aims

Specific Aim 1: To explore *Sfrp4* deletion effects on alveolar bone.

Hypothesis: Lack of *Sfrp4* results in reduced bone volume, thin cortical bone, and thick trabecular bone in alveolar bone area.

Specific Aim 2: To determine whether *Sfrp4* deletion affects healing of tooth extraction socket.

Hypothesis: Lack of *Sfrp4* impairs bone regeneration and healing in tooth extraction socket.

Understanding the mechanism by which Sfrp4 and therefore Wnt signaling affect alveolar bone healing may provide insights into the development of novel and specific therapeutic approaches to accelerate alveolar bone healing.

1.3 Background

Wnt ligands are signaling proteins that belong to a family of glycosylated-lipid-modified proteins (Logan, Nusse 2004). Wnt signaling pathway is highly related to bone development and bone homeostasis as well as bone repair and regeneration (Baron, Kneissel 2013; Gori, Baron 2013). Nineteen Wnt proteins has been identified (Tamura, Nemoto, Sato et al. 2010; Gori, Baron 2013). Wnt signaling is classically divided into canonical Wnt pathway and non-canonical Wnt pathway (Figure 2).

In canonical Wnt pathway, Wnt ligands bind to dual receptor complexes of frizzled receptors and low-density lipoprotein receptor-related proteins (LRP5/6) co-receptors to initiate Wnt-β-catenin signaling. This process prevents degradation of β-catenin and allows for β-catenin accumulation and translocation into the nucleus to initiate transcription of Wnt target genes. Canonical Wnt signaling activation increases bone mass and enhances osteoblast differentiation and indirectly represses osteoclast differentiation and bone resorption (Baron, Kneissel 2013; Gori, Baron 2013; Majidinia, Sadeghpour, Yousefi 2017). Because of that, activation of canonical Wnt signaling has been used as a therapeutic aid to increase bone mass and favor fracture healing. On the other hand, non-canonical Wnt signaling activates alternative pathways like the Wnt/planar cell polarity (PCP), the Wnt/Ca^{+2}, Wnt/JNK, and Wnt/Ror. It functions by binding to frizzled receptors alone or with other receptors independent of β-catenin like Ror2 or Ryk. Activation of non-canonical Wnt signaling stimulates osteoclast differentiation and is involved in bone remodeling (Baron, Kneissel 2013; Gori, Baron 2013; Chen, Ng, Chen et al. 2019). Activation of non-canonical Wnt signaling can act as a positive regulator of osteoblast differentiation and

prevent apoptosis of osteoblast progenitors and differentiated osteoblasts (Majidinia, Sadeghpour, Yousefi 2017), but can also lead to improper cortical bone mass as in Pyle disease patients (Kiper, Saito, Gori et al. 2016). There are multiple Wnt antagonists which inhibits Wnt signaling by either binding to Wnt receptors like Dickkopf1 (Dkk1) and sclerostin (Sost) or binding to Wnt ligands like sFRPs and Wnt inhibitory factor-1 (Wif-1) (Baron, Kneissel 2013; Gori, Baron 2013) (Figure 2).

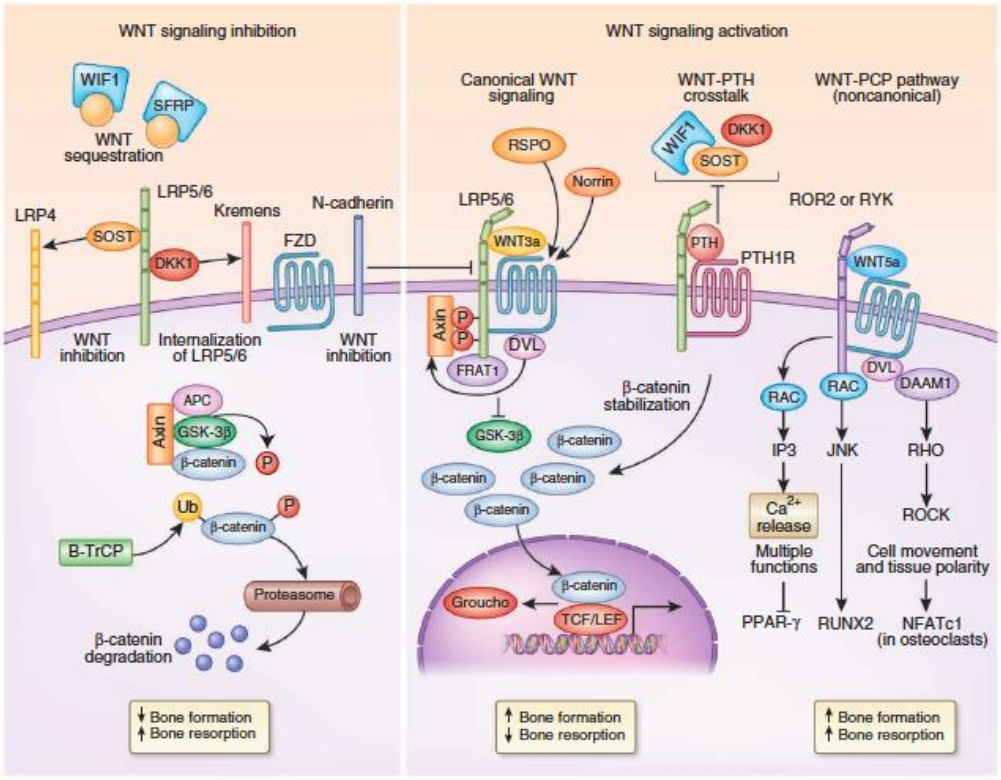

Figure 2: Wnt signaling. Activation and inhibition processes of different Wnt pathways (Baron, Kneissel 2013)

Pyle's disease is a rare skeletal disease characterized by increased trabecular bone, thin cortex in long bones and increased fracture susceptibility (Pyle 1931; Heselson, Raad, Hamersma et al. 1979; Beighton 1987; Kiper, Saito, Gori et al. 2016). Our lab has shown that Pyle disease is caused by loss-of-function mutations in the gene encoding secreted frizzled-related protein 4 (sFRP4) (Kiper, Saito, Gori et al. 2016). sFRP family (sFRP1 to 5) are Wnt antagonists that interfere with Wnt ligands and receptor complexes interactions which in turn lead to inhibition of

both canonical and non-canonical Wnt signaling pathways (Gori, Baron 2013; Chen, Ng, Chen et al. 2019) (Figure 3). Genome wide studies (GWAS) have showed that sFRP4 is associated to bone mineral density (Styrkarsdottir, Halldorsson, Gretarsdottir et al. 2008; Cho, Go, Kim et al. 2009). Our investigations have demonstrated that in mice, while *Sfrp4* deficiency activates canonical Wnt signaling in trabecular bone, leading to increased trabecular bone mass, it activates both canonical and non-canonical Wnt cascades in cortical bone and the activation of non-canonical cascade which leads to reduced cortical bone thickness (Kiper, Saito, Gori et al. 2016).

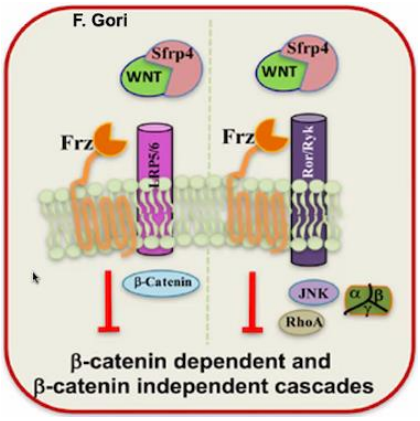

Figure 3: Sfrp4 inhibits both canonical (β-catenin dependent) and non-canonical (β-catenin independent) cascades by functioning as a decoy receptor for the Wnt ligands.

Beside the known anabolic role of canonical Wnt signaling activation in the axial skeleton, Wnt signaling is also important for periodontal ligament and alveolar bone homeostasis. Inactivation of the Wnt signals results in a significant reduction in alveolar bone volume and density (Yin, Li, Salmon et al. 2015). It has been shown that activation of Wnt signaling results in narrowing of periodontal ligament space while down regulation of Wnt signaling causes widening of periodontal ligament space (Lim , Liu, Mah et al. 2015) and disorganized periodontal ligament fibers (Yin, Li, Salmon et al. 2015). Moreover, it has been demonstrated that Wnt-responsive cells are associated with higher rate of bone formation and faster healing of osteotomy in alveolar bone (Li, Yin, Huang et al. 2017). The same study indicated positive correlation between Wnt signaling and implant osseointegration and showed that most of the new bone formation around implants arises from Wnt-resposive cells (Li, Yin, Huang et al. 2017).

Alveolar bone around teeth consists of both trabecular and cortical bone. Tooth extraction, a routine clinical procedure, is often associated with alveolar bone loss (Araújo, Silva, Misawa et al. 2015; Chappuis, Araújo, Buser 2017). Both quality and quantity of healed extraction socket sites have huge impact on dental implants successfulness (Avivi-Arber, Avivi, Perez et al. 2018). The healing process of the extraction socket involves both bone formation and bone resorption. This process starts with inflammatory cell migration to the extraction site. After that, recruited osteoblasts start woven bone formation to fill the socket. Finally, bone remodeling occurs to replace woven bone with lamellar bone (Araújo, Silva, Misawa et al. 2015; Jiang, Yang, Meng et al. 2019). Most of bone resorption occurs in the facial site of alveolar bone which is presented as a thin bone plate (Araújo, Silva, Misawa et al. 2015; Chappuis, Araújo, Buser 2017). Socket healing after extraction exhibits dimensional changes in the alveolar ridge. Indeed, up to 50% reduction in alveolar ridge dimension with substantial horizontal reduction and less vertical reduction has been reported (Araújo, Silva, Misawa et al. 2015).

Cortical bone mass is a main determinant of bone strength and fracture susceptibility. With aging, cortical bone thickness decreases and fragility increases leading to bone fracture. As in physiologic aging, osteoporotic patients present with thin cortical bone and increased fracture risk (Liu, Li, Arioka et al. 2019). A delay in alveolar bone healing is also seen with aging and osteoporotic-like conditions in mice (Liu, Li, Arioka et al. 2019). It is therefore possible that diseases that present with thin cortical bone phenotype result in more dimensional changes and delayed alveolar bone healing after tooth extraction. Impaired tooth extraction socket healing and increased dimensional changes in alveolar ridge negatively affects future implant treatment and make it more complex to replace missing teeth which leads to esthetic and functional challenges in the oral cavity.

As for long bones, *Sfrp4* deficiency might similarly affect alveolar bone: thin and fragile cortical bone and expanded trabecular bone. However, alveolar bone in *Sfrp4* deficient mice and in Pyle's disease has not been studied. It is not known whether deletion of this secreted protein has effects on the extraction socket healing time, quality and quantity of bone filling the socket. So, the overall aim of this study is to explore the effects of *Sfrp4* deletion on alveolar bone and healing of tooth extraction using our mouse model of Pyle's disease.

2 Methods

2.1 Animals

For all studies *Sfrp4+/-* mice were interbred to obtain *Sfrp4+/+* (*wild type*), *Sfrp4+/-* and *Sfrp4-/- (Sfrp4* knock out) mice. Eight week-old male and female *Sfrp4* knock out (KO) and their *wild type* littermates were used. Six mice per group/time point were analyzed. All animals are in the C57/BL6 background and are housed in the Harvard Center for Comparative Medicine. Animal studies were approved by the Harvard University Institutional Animal Care and Use Committee.

2.2 Tooth extraction model

Mice were anesthetized by intraperitoneal administration of ketamine (100 mg/ml) and xylazine (100 mg/ml). The maxillary right incisor was extracted. Before extraction, the mouth was rinsed with sterile saline. Maxillary right incisor was gently luxated using a disposable guage-18 needle as an elevator and then extracted using a micro-forceps with aid of magnifying loupes (Avivi-Arber, Avivi, Perez et al. 2018; Strauss, Stähli, Kobatake et al. 2020) (Figure 4). Bleeding was controlled by applying light compression on the extraction sites without suturing. Sites of alveolar bone plate or tooth fracture were excluded from the study. Buprenorphine injection was used twice daily for two consecutive days after the surgeries. Mice were fed with soft food after extraction to ensure proper soft tissue healing.

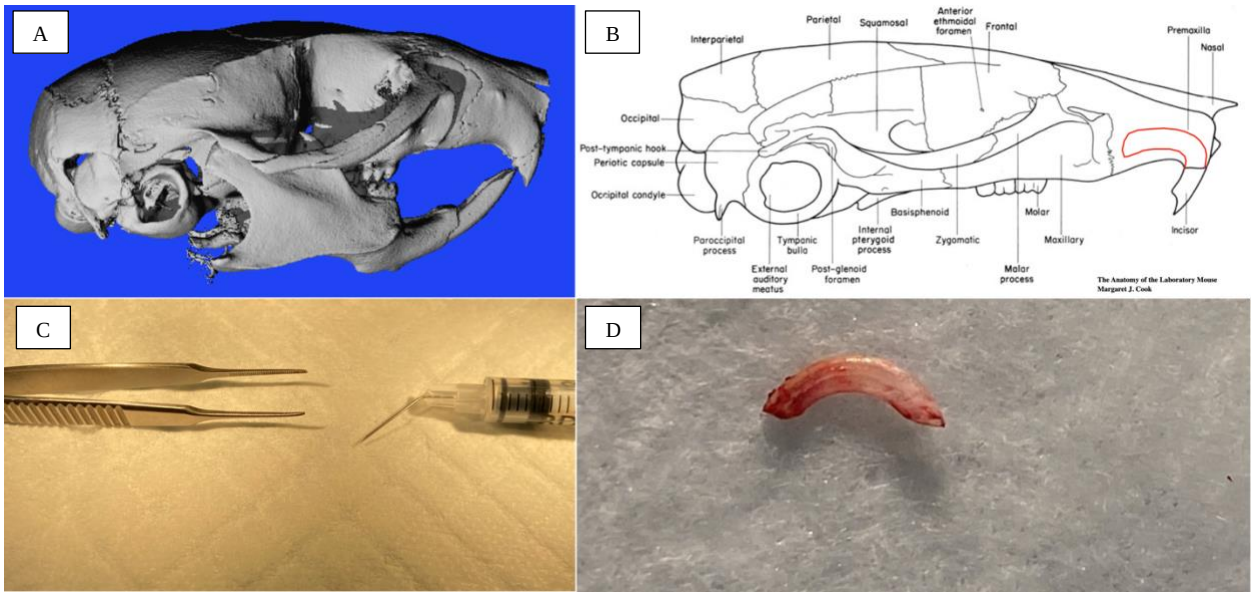

Figure 4: Tooth extraction procedure.

A) Representative lateral view of 3D reconstruction of mouse skull. B) Schematic lateral view of a mouse skull showing the outline of maxillary incisor alveolar socket (Red) (Source: Cook, Margaret J. The Anatomy of the Laboratory Mouse). C) Tools used for tooth extraction: Disposable needle with micro-forceps. D) Extracted maxillary incisor.

2.3 Study design

Animals were sacrificed by CO_2 intoxication, one week (E1), two weeks (E2), and three weeks (E3) after tooth extraction. Mice were intraperitoneally injected with 20 mg/kg of calcein at 7 days and 10 mg/kg of calcein with 40 mg/kg of demeclocycline at 2 days prior to sacrificing to allow for dynamic bone histomorphometric analysis (Figure 5, Table 1). Skulls were harvested for three-dimensional micro-computed tomography and bone histomorphometry.

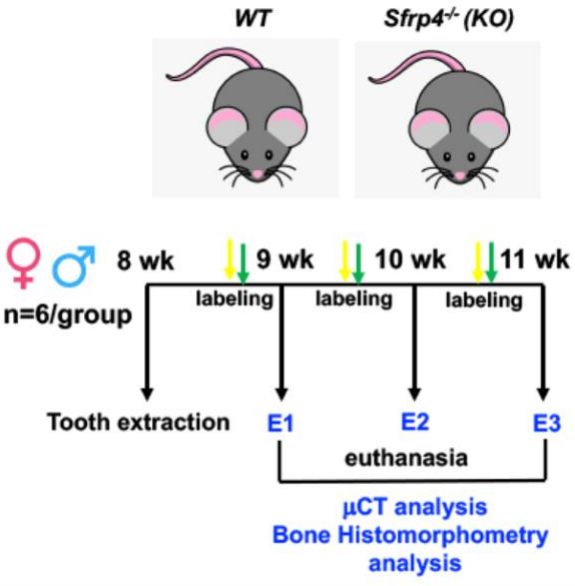

Figure 5: Schematic illustration of the study design.

Time Point	**E1**		**E2**		**E3**	
Genotype	*WT*	*Sfrp4 KO*	*WT*	*Sfrp4 KO*	*WT*	*Sfrp4 KO*
Gender	Male and Female		Male and Female		Male and Female	
Age of surgery	8 week-old		8 week-old		8 week-old	
1st Injection	Calcein 7 days before sacrifice		Calcein 7 days before sacrifice		Calcein 7 days before sacrifice	
2nd Injection	Demeclocycline+Cacein 2 days before sacrifice		Demeclocycline+Cacein 2 days before sacrifice		Demeclocycline+Calcein 2 days before sacrifice	
Analysis	μCT, histomorphometry		μCT, histomorphometry		μCT, histomorphometry	
Age of euthanasia	1 week after extraction 9 week-old		2 week after extraction 10 week-old		3 weeks after extraction 11 week-old	

Table 1: Study Design

2.4 Three-dimensional micro-computed tomography assessment

After necropsy, dissected skulls were fixed in 70% ethanol with three changes at 4°C. Three-dimensional micro-computed tomographic scanning (μCT) was performed for all groups at all time points using a high-resolution desktop microtomographic imaging system (μCT35, Scanco Medical AG, Brüttisellen, Switzerland). Scans were acquired using a 10 μm^3 isotropic voxel size, 70 kVP, 114 μA, and 200 ms integration time. Images were subjected to Gaussian filtration and segmented using a fixed threshold of 700 $mgHA/cm^3$. Analysis followed the published guidelines (Bouxsein, Boyd, Christiansen et al. 2010). Bone morphometry and 3D reconstruction for region of interests were carried out (Figure 6).

Figure 6: Representative frontal view of 3D reconstruction of mouse skull after extraction of the maxillary right incisor.

To explore the effect of *Sfrp4* deletion on the alveolar bone, Three regions of interest (ROI) were analyzed. The first ROI is the lateral and medial part of the bone plate around the maxillary left incisor (contra-lateral tooth). The first ROI is an axis length of 1 mm (50 slices) in the middle part of alveolus in apical-coronal direction. The superior-inferior limit was aligned with the superior and the inferior height of the contour of the tooth. The contours were selected manually for each slice. Bone in the region of interest was segmented. Bone volume fraction (BV/TV) was measured (Figure 7).

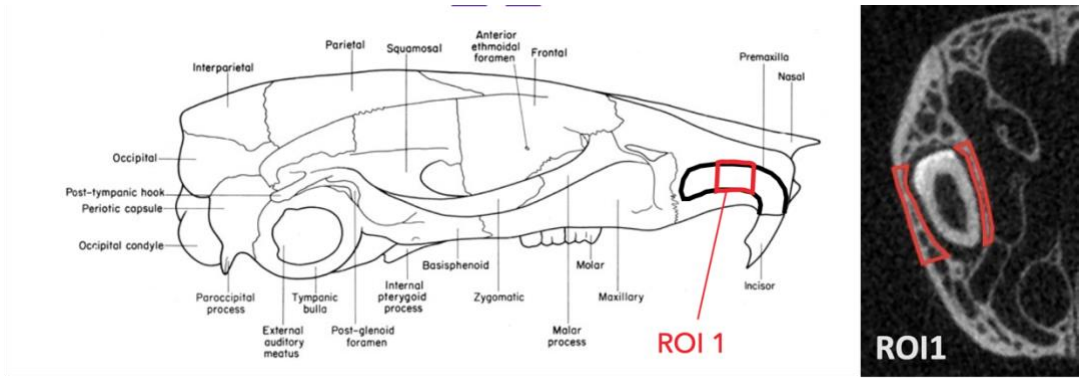

Figure 7: Schematic lateral view of skull (left) and coronal section of skull μCT (right) showing the first ROI in lateral and medial part of the alveolar bone plate around the maxillary left incisor (red) to be analyzed.

The second ROI is the alveolar bone area superior to the maxillary left incisor (Figure 8). This ROI is an axis length of 1 mm (50 slices) in the middle part of alveolus in apical-coronal

direction. Alveolar bone in the region of interest was segmented. BV/TV and porosity were measured. Porosity is the percentage of void areas within ROI in relation to the total area of ROI.

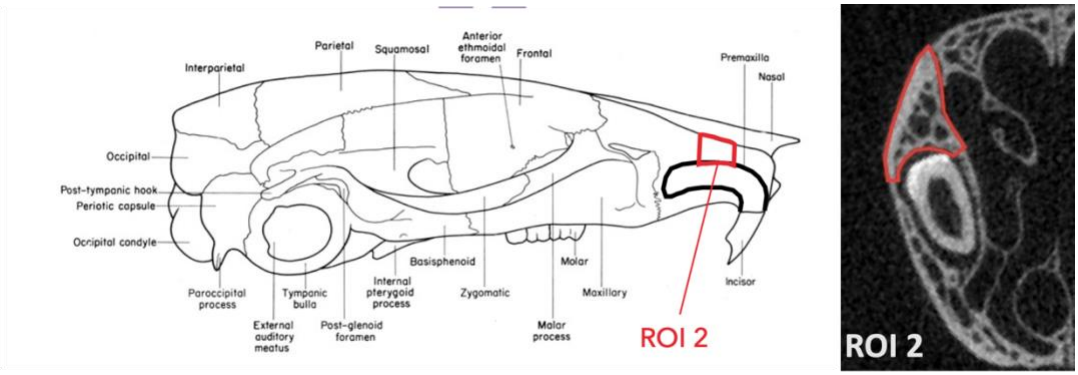

Figure 8: Schematic lateral view of skull (left) and coronal section of skull μCT (right) showing the second ROI in the alveolar bone area superior to maxillary left incisor (red) to be analyzed.

The third ROI is the alveolar bone area around maxillary left molars (Figure 9). This ROI is an axis length of 1 mm (50 slices) starting from the anterior end of malar process of zygomatic arch and extending posteriorly. Alveolar bone in the region of interest was segmented. BV/TV and porosity were be measured.

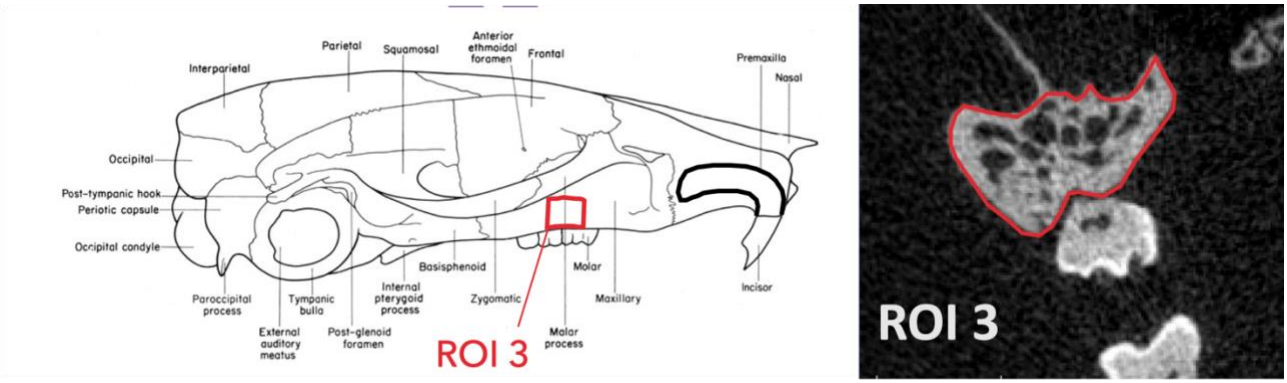

Figure 9: Schematic lateral view of skull (left) and coronal section of skull μCT (right) showing the third ROI in alveolar bone area around maxillary left molars (red) to be analyzed.

To determine whether *Sfrp4* deletion affects healing of incisor tooth extraction socket, the healing socket of the extracted maxillary right incisor was analyzed. The ROI is an axis length of 1 mm (50 slices) in the middle part of alveolus in apical-coronal direction (Figure 10). Bone volume fraction (BV/TV), trabecular number (Tb.N), trabecular thickness (Tb.Th), trabecular separation (Tb.Sp), and bone mineral density (BMD) were measured. Analysis was performed at one week (E1), two weeks (E2), and three weeks (E3) after teeth extraction.

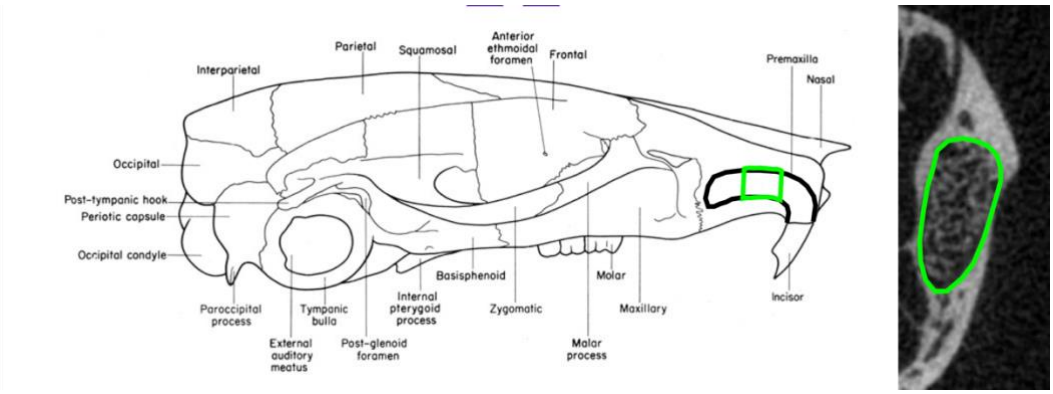

Figure 10: Schematic lateral view of skull (left) and coronal section of skull μCT (right) showing the ROI in extracted maxillary right incisor socket (Green) to be analyzed.

2.5 Bone histomorphometric analysis

After μCT analysis was performed, the right half of the skull was harvested and crowns of maxillary molars were amputated. Specimens were dehydrated with graded acetone and embedded in methyl methacrylate. Undecalcified skulls with tooth socket sections were cut at 5 μm thickness in a plane parallel to the skull sagittal suture by microtome (RM2255 Microtome, Leica Biosystems, Germany). The sections from the central region of tooth socket were analyzed.

To determine whether *Sfrp4* deletion affects healing of tooth extraction socket, the healing socket of the extracted maxillary right incisor was analyzed. Sections were stained with Von Kossa to identify mineralized bone. The standardized ROI for all histomorphometric analyses is a rectangular area (0.9X1.3mm). The ROI is in the middle part of alveolus in apical-coronal direction (Figure 11).

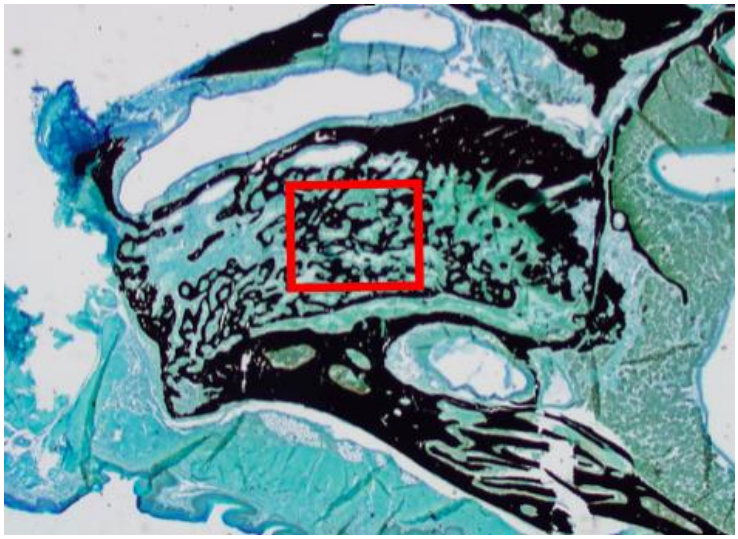

Figure 11: Representative photomicrograph of Von Kossa stained section of maxillary incisor extraction socket after 3 weeks of healing showing the standardized ROI for all histomorphometric analyses (Red) to be analyzed.

For dynamic analysis, newly formed bone within the extraction sockets were analyzed. Under florescence, the section shows double labeling of calcein and demeclocycline with calcein. The area between the two labels is determined as the area of newly formed bone. Mineral apposition rate (MAR), bone formation rate per unit of bone surface (BFR/BS), Bone formation rate per unit of bone volume (BFR/BV) were measured. For cellular analysis, sections were stained with 2 % Toluidine blue for the analysis of osteoblasts. Osteoblast surface per bone surface (Ob.S/BS) and osteoblasts number per bone perimeter (Ob.N/B.pm) were calculated. Sections were stained with Tartrate-resistant acid phosphate (TRAP) for the analysis of osteoclasts. The surface of osteoclasts relative to the bone surface (Oc.S/BS) and osteoclasts number per bone

perimeter (Oc.N/B.pm) were calculated. BV/TV was obtained by taking the average of 3 distinct histomorphometric measurements from consecutive sections.

The sections were viewed using a motorized microscope (Nikon E800, Nikon Instruments Inc., NY, USA) equipped with a digital camera (Olympus DP71, Olympus Corporation, PA, USA). Image captures were performed using CellSens software (Olympus Corporation, PA, USA) under 2X and 20X magnification. The bone histomorphometric data was obtained at 100X magnification, in ROI inside the tooth socket. The OsteoMeasure analyzing software (Osteometrics Inc., Decatur, GA, USA) was used to generate and calculate the data. The parameters were presented according to the standardized nomenclature (Dempster, Compston, Drezner et al. 2013).

2.6 Statistical analysis

To compare the alveolar bone between *WT* and *Sfrp4 KO* groups, descriptive statistics (means, $\pm$ standard deviations) were calculated. Statistical significance was assessed using the students' t- test. To compare the socket healing after tooth extraction between *WT* and *Sfrp4 KO* mice at different time points (E1, E2, E3), descriptive statistics were calculated. At each time point, statistical significance was assessed using the students' t- test. Significance was attained at $p < 0.05$ (*), $p < 0.01$ (**), $p < 0.001$ (***), $p < 0.0001$ (****). All statistical analysis were performed using GraphPad Prism 9.0 (GraphPad Software Inc., San Diego, CA, USA).

3 Results

3.1 *Sfrp4* deletion results in decreased bone volume and increased porosity in alveolar bone

Our first aim was to explore *Sfrp4* deletion effects on alveolar bone in maxillary incisor and molars areas. To this end, μCT analysis was performed for *WT* and *Sfrp4* KO mice at 10 and 11 weeks. Compared to *WT* mice, *Sfrp4* KO mice exhibited structural changes in alveolar bone architecture. Alveolar bones in *Sfrp4* KO mice presented with increased trabeculation and thinning of cortical bone. Similar to the skeletal phenotype in Pyle's disease patients and in our mouse model, no difference were observed between males and females (Kiper, Saito, Gori et al. 2016).

μCT analysis showed that medial and lateral bone plate around the maxillary left incisor (ROI 1) in *Sfrp4 KO* has reduced bone volume fraction (BV/TV=58.47% ±7.84) compared to *WT* mice (BV/TV=77.92% ±8.36) (Figure12 A, B). The superior part of incisor alveolar bone (ROI 2) also showed less bone volume fraction with more porosity in *Sfrp4 KO* group (BV/TV=86.16% ±3.79, Porosity=0.93% ±1.00 in *WT* group; BV/TV=71.60% ±11.76, Porosity=12.33% ±9.36 in *Sfrp4 KO* group) (Figure12 A, C). Similar to the incisor alveolar bone, molars alveolar bone (ROI 3) presented with reduced bone volume fraction and increased porosity in *Sfrp4 KO* group (BV/TV=81.44% ±3.45, Porosity=9.89% ±2.63 in *WT* group; BV/TV=75.44% ±2.97, Porosity=17.59% ±3.51 in *Sfrp4 KO* group) (Figure12 D, E).

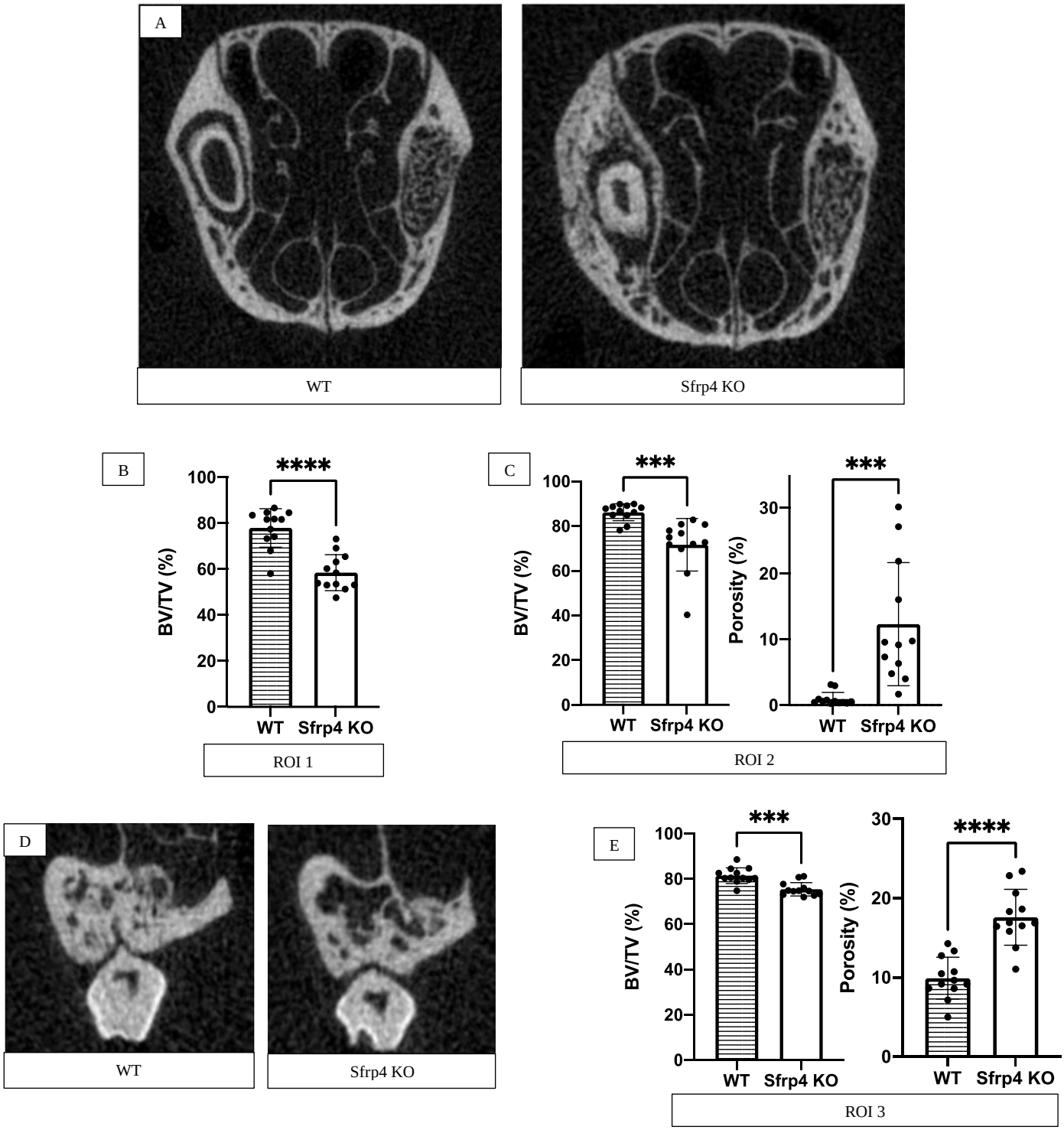

Figure 12: µCT analysis of alveolar bone in maxillary incisor and molars areas.

Representative µCT images of skulls showing the structural difference in maxillary incisor alveolar bone (A) and maxillary molars alveolar bone (D) between *WT* and *Sfrp4 KO* mice in coronal view. µCT assessment of BV/TV of ROI 1 (B), BV/TV and porosity of ROI 2 (C), BV/TV and porosity of ROI 3 (E) showing significantly decreased BV/TV and increased porosity in *Sfrp4 KO* group compared to *WT* group. Data (means, ±SD). $p < 0.001$ (***), $p < 0.0001$ (****).

3.2 *Sfrp4* deletion does not have a significant effect on socket bone healing after incisor tooth extraction

μCT analysis showed no new bone in the alveolar socket at one week after incisor extraction (E1) in both *WT* and *Sfrp4 KO* groups (Figure 13A). Because of that, no statistical analysis was done at E1 time point. At E2 time point, *WT* and *Sfrp4 KO* groups showed no significant difference in bone healing of alveolar socket (Table 2, Figure 13A, B). All bone parameters BV/TV, Tb.N, Tb.Th, Tb.Sp, BMD) were not significantly different between groups. Similarly, no statistically significant difference in all bone parameters was detected in the healing sockets at E3 time points (Table 2, Figure 13A, C). As anticipated, BV/TV, Tb.N, Tb.Th, BMD markedly increased and Tb.Sp decreased from E2 to E3 time points in both groups indicating that the amount of bone formation increases over time. (Table 2, Figure13D).

	E2		E3	
	WT	*Sfrp4 KO*	*WT*	*Sfrp4 KO*
BV/TV (%)	38.96 (±5.19)	40.85 (±5.68)	57.70 (±6.24)	62.20 (±8.91)
Tb.N (1/mm)	7.44 (±1.36)	6.74 (±1.32)	8.94 (±1.28)	8.41 (±0.92)
Tb.Th (mm)	0.069 (±0.009)	0.072 (±0.010)	0.084 (+0.017)	0.094 (±0.016)
Tb.Sp (mm)	0.143 (±0.036)	0.155 (±0.039)	0.099 (±0.018)	0.108 (±0.032)
BMD (mg HA/cm^3)	530.7 (±29.2)	540.5 (±33.4)	571.7 (±31.4)	581.1 (±16.43)

Table 2: Bone microarchitecture from μCT analysis of the tooth extraction socket healing at 2 weeks after extraction (E2) and 3 weeks after extraction (E3). Data: mean (±SD).

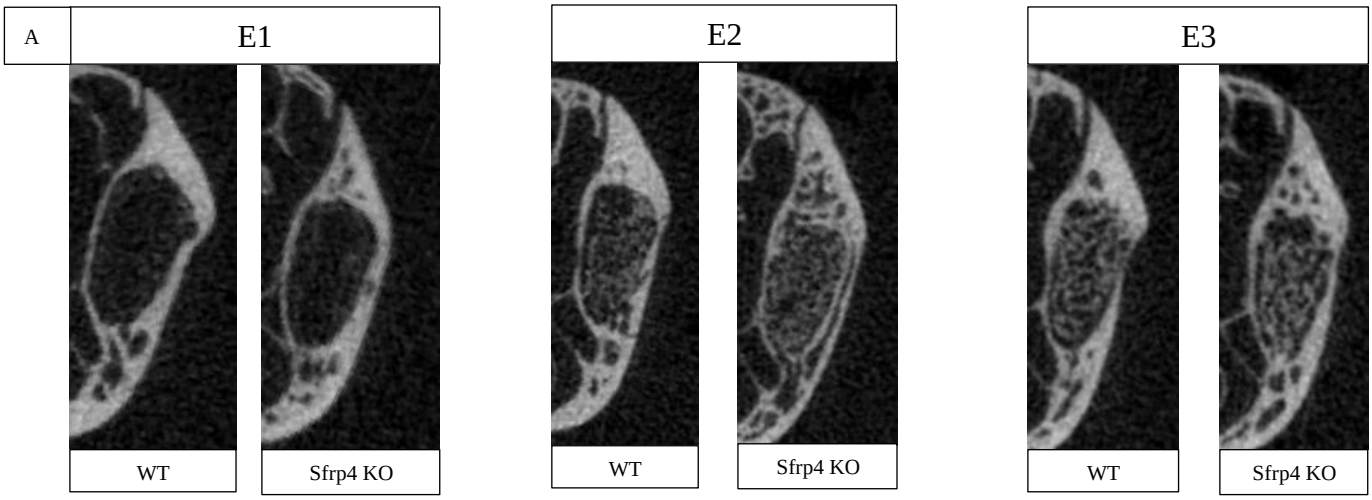
A
E1
E2
E3
WT
Sfrp4 KO
WT
Sfrp4 KO
WT
Sfrp4 KO

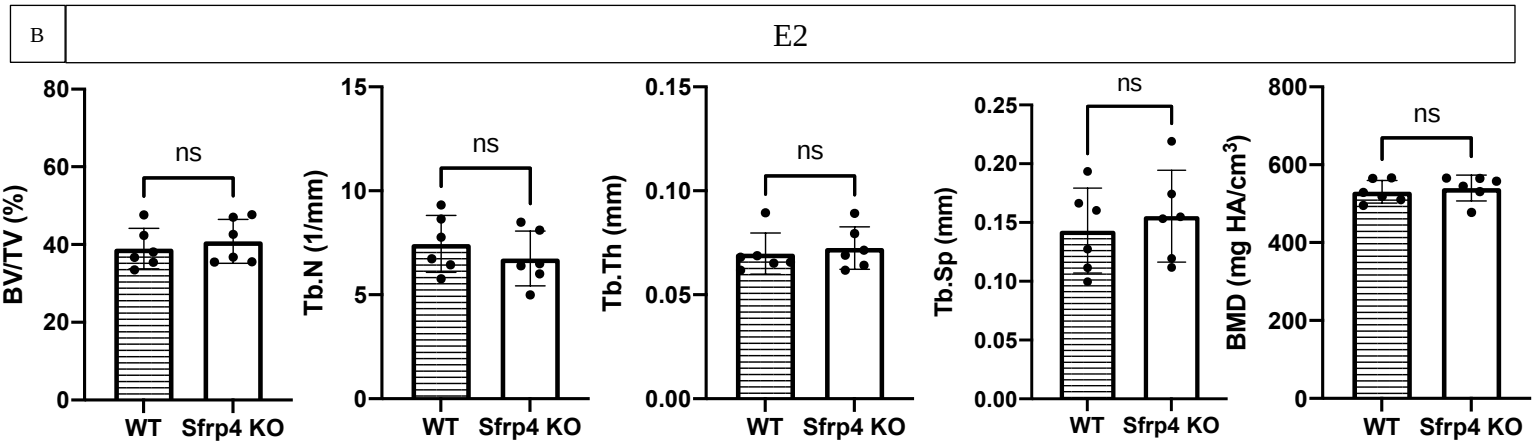
B
E2
BV/TV (%)
Tb.N (1/mm)
Tb.Th (mm)
Tb.Sp (mm)
BMD (mg HA/cm3)
ns
WT
Sfrp4 KO

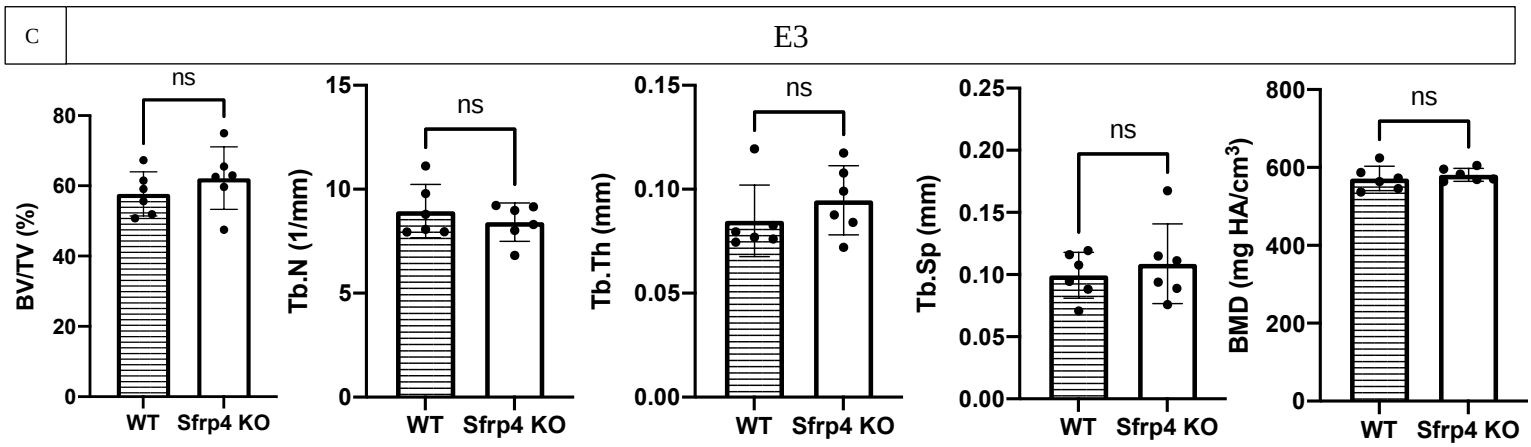
C
E3
BV/TV (%)
Tb.N (1/mm)
Tb.Th (mm)
Tb.Sp (mm)
BMD (mg HA/cm3)
ns
WT
Sfrp4 KO

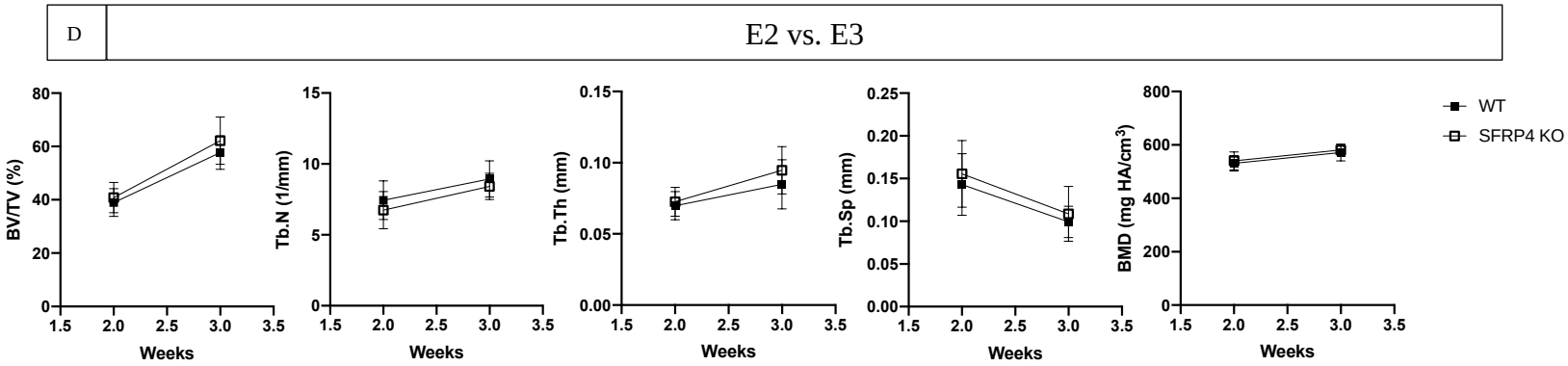

Figure 13: µCT analysis of alveolar socket healing after tooth extraction.

A) Representative µCT images of tooth extraction socket at E1, E2, E3 timepoints in coronal view.

B, C) µCT assessment of BV/TV, Tb.N, Tb.Th, Tb.Sp, BMD of tooth extraction socket at 2 weeks after extraction (E2) and 3 weeks after extraction (E3) showing similar results in both *WT* and *Sfrp4 KO* groups.

D) µCT assessment at E3 compared to E2 showing BV/TV, Tb.N, Tb.Th, BMD markedly increased and Tb.Sp decreased from E2 to E3 time points in both *WT* and *Sfrp4 KO* groups.

Data (mean, ±SD). ns: non statistically significant difference ($p > 0.05$).

Histomorphometric analysis was performed at E3 time point. The results of histomorphometric data confirm the µCT analysis. Von Kossa stained sections showed that trabecular bone filled most of the alveolar socket in both *WT* and *Sfrp4 KO* groups (Figure 14A, B). Fluorescent micrographs illustrating fluorochrome labels were used for dynamic histomorphometric analysis (Figure 14C, D). Five days interval of calcein (7 days before sacrifice) and demeclocycline with calcein (2 days before sacrifice) injections resulted in double fluorochrome labelling and allowed for measuring the daily rate of new bone formation. Both *WT* and *Sfrp4 KO* groups showed double labelling throughout the alveolar socket which indicate active bone formation during the healing process (Figure 14C, D). All dynamic bone histomorphometric parameters showed similar rate in both *WT* and *Sfrp4 KO* groups (MAR=1.93 ±0.14 in *WT*,

MAR=2.02 ±0.21 in *Sfrp4 KO*; BFR/BS=0.73 ±0.21 in *WT*, BFR/BS=0.72 ±0.12 in *Sfrp4 KO*; BFR/BV=3.10 ±0.94 in *WT*, BFR/BV=3.22 ±0.48 in *Sfrp4 KO*) (Figure 14I).

Cellular histomorphometric analysis was performed to evaluate the number of osteoblasts and osteoclasts in the alveolar socket (Figure 14E-H). *Sfrp4 KO* alveolar sockets showed a slight decrease in osteoblasts number and a slight increase in osteoclasts number compared to *WT* alveolar sockets but these changes were not statistically significant (Figure 14J). Average bone volume fraction from all previous dynamic and cellular histomorphometric analyses indicated a similar BV/TV in alveolar sockets of both *WT* and *Sfrp4 KO* groups (BV/TV=47.24% ±3.83 in *WT*, BV/TV=50.42% ±3.60 in *Sfrp4 KO*) (Figure 14I).

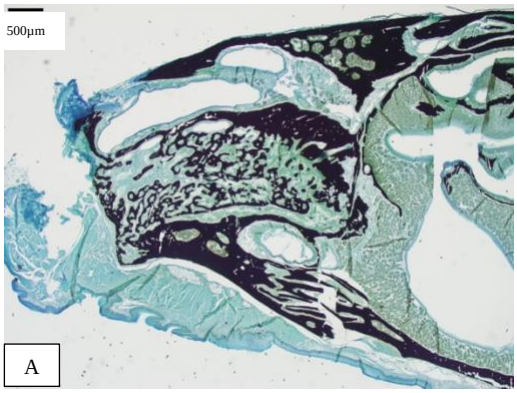

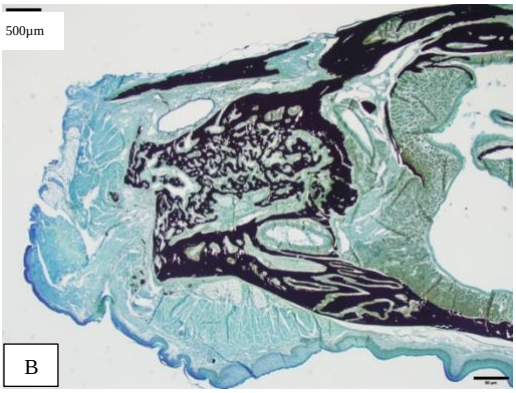

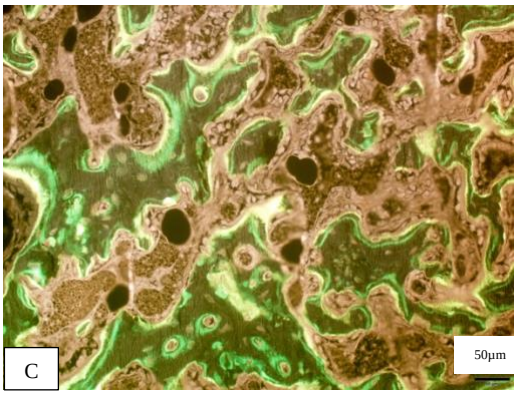

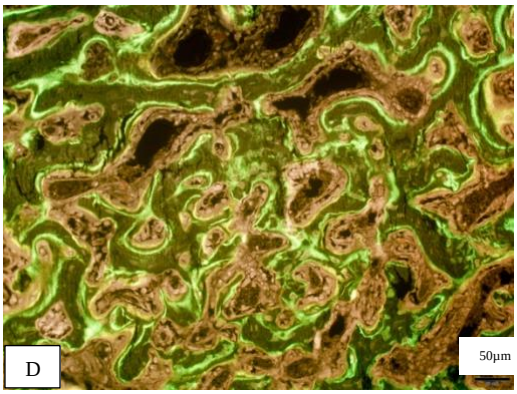

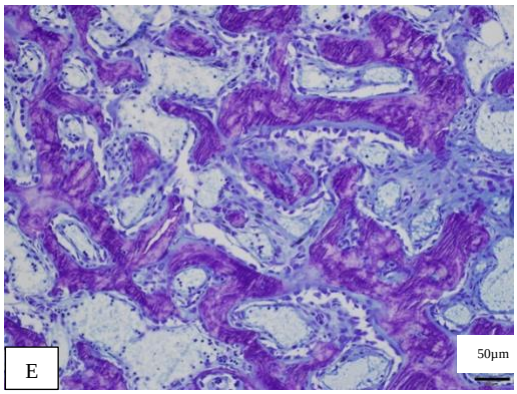

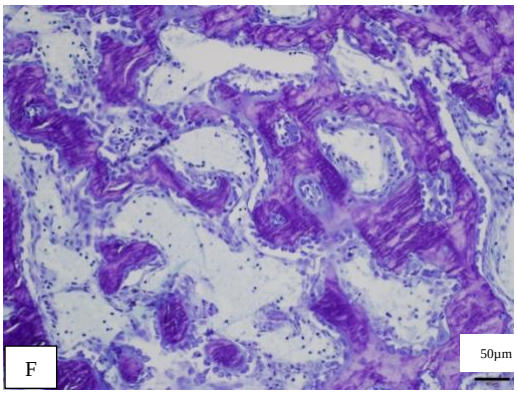

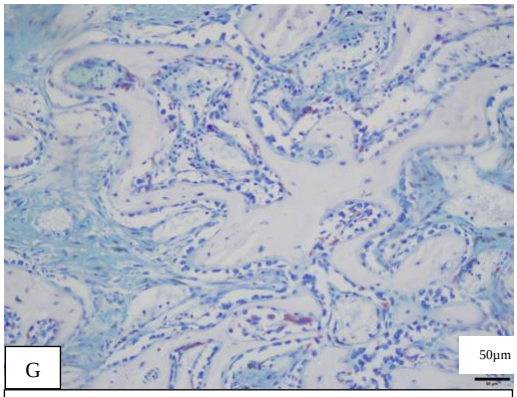

WT

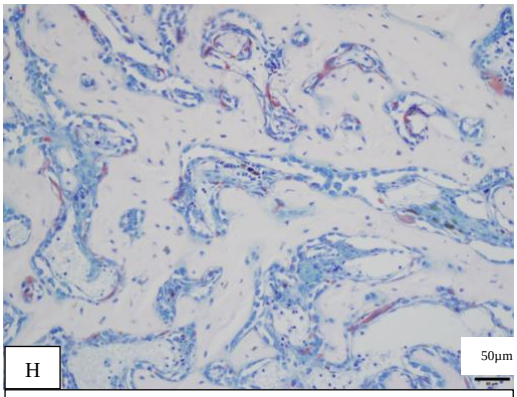

Sfrp4 KO

I

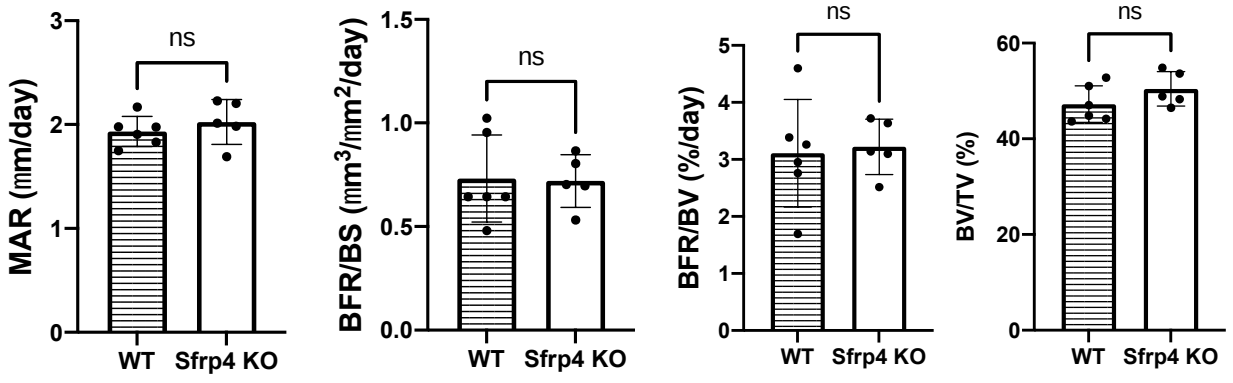

J

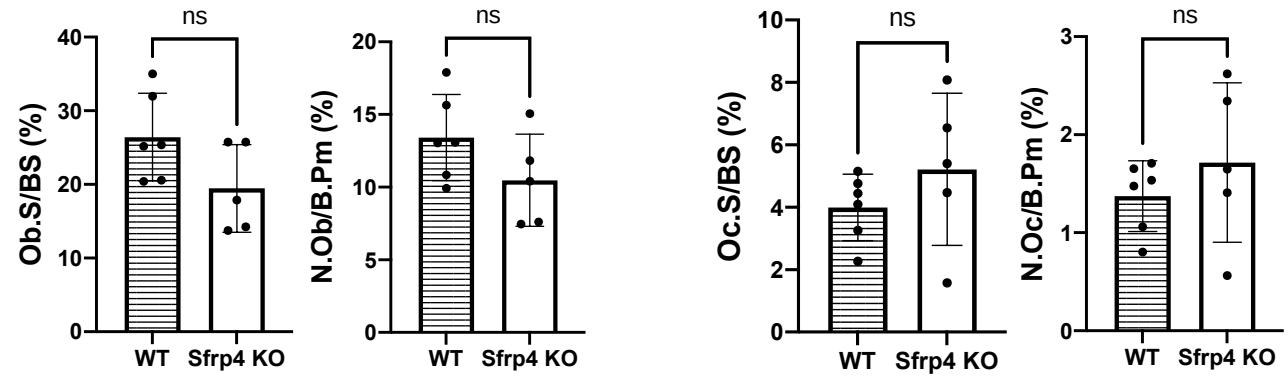

Figure 14: Histomorphometric analysis of alveolar socket healing after tooth extraction at E3 time point.

A-H) Representative photomicrographs of histological section of tooth extraction socket. Von Kossa stained sections showing trabecular bone filling the alveolar socket in both *WT* and *Sfrp4 KO* groups (A, B). Unstained sections under fluorescent light showing double labelling in newly formed bone throughout the alveolar socket in both *WT* and *Sfrp4 KO* groups (C, D). Sections stained with toluidine blue showing osteoblasts (blue) surrounding newly formed bone (purple) in healing sockets of *WT* and *Sfrp4 KO* groups (E, F). Sections stained with TRAP showing osteoclasts (purple surrounding newly formed bone (white) in healing sockets of *WT* and *Sfrp4 KO* groups (G, H). (Left: WT, Right: Sfrp4 KO).

I) Dynamic histomorphometric assessment parameters showing comparable mineral apposition rate and bone formation rate in healing sockets of *WT* and *Sfrp4 KO* groups and structural histomorphometric assessment showing comparable BV/TV rate in healing sockets of *WT* and *Sfrp4 KO* groups at E3 timepoint.

J) Cellular histomorphometric Assessment parameters showing a slight decrease in osteoblasts number (Ob.S/BS, N.Ob/B.Pm) and a slight increase in osteoclasts number (Oc.S/BS, N.Oc/B.Pm) compared to *WT* alveolar sockets but these changes were not statistically significant.

Data (mean, ±SD). ns: non statistically significant difference ($p > 0.05$)

4 Discussion

4.1 sFRP4 is essential for proper alveolar bone homeostasis

Wnt signaling is important for alveolar bone homeostasis. It has been shown that inactivation of the Wnt signals results in a significant reduction in alveolar bone volume and density (Yin, Li, Salmon et al. 2015). sFRP4 is a Wnt antagonist that interferes with Wnt ligands and in turn leads to inhibition of both canonical and non-canonical Wnt signaling pathways. Therefore, its deletion results in activation of canonical and non-canonical Wnt signaling cascades (Gori, Baron 2013; Chen, Ng, Chen et al. 2019). Our μCT analysis showed that *Sfrp4* deletion leads to reduced bone volume and increased porosity in the incisor and molars alveolar bone areas. It has been shown that deletion of Sclerostin (Sost), a Wnt antagonist which differently from Sfrp4 binds to LRP5/6 receptors to inhibit canonical Wnt signaling only (Baron, Kneissel 2013; Gori, Baron 2013), results in increased bone volume and reduced porosity in alveolar bone (Kuchler, Schwarze, Dobsak et al. 2014). Thus, our findings suggest that non-canonical Wnt signaling might be the main factor affecting alveolar bone in *Sfrp4* mutant mice.

Previous studies in our lab indicated that deletion of *Sfrp4* activates predominantly canonical Wnt signaling in trabecular bone, and activates both canonical and non-canonical Wnt signaling in cortical bone (Kiper, Saito, Gori et al. 2016). Consequently, *Sfrp4 KO* mice presents with increased trabecular bone mass and thin cortical plates in long bone. These results are in agreement with our finding as *Sfrp4* deletion resulted in less bone volume and more trabecular space in alveolar bone of incisor and molars areas.

4.2 Alveolar bone phenotype and tooth extraction socket healing

Tooth extraction socket healing is affected by alveolar bone phenotype. In a socket healing study, it has been demonstrated that aged and ovariectomized (OVX) young mice exhibited less

bone volume fraction and more trabecular space in alveolar bone compared to young mice (Liu, Li, Arioka et al. 2019). When socket healing was evaluated after maxillary molar tooth extraction, aged and OVX mice produced less bone volume fraction even after complete healing of the socket (Liu, Li,Arioka et al. 2019). In the present study, although *Sfrp4* deletion resulted in reduced alveolar bone volume and increased porosity, the socket bone healing after extraction was not different than *WT* animals. One difference in bone phenotype between OVX and *Sfrp4* mutant mice is the trabecular bone mass. The trabecular bone mass is decreased in OVX and aged mice, while it is increased in *Sfrp4* mutant mice (Kiper, Saito, Gori et al. 2016; Chen, Ng, Chen et al 2019; Zhou, Wang, Qiao et al. 2018). These findings suggest that trabecular bone mass play a major role in socket healing.

4.3 Different Wnt signaling cascades and tooth socket healing

Wnt signaling is essential for socket healing. It has been demonstrated that Wnt-responsive cells are associated with higher rate of bone formation and faster healing of osteotomy in alveolar bone (Li, Yin, Huang et al. 2017). Along with Sost, Dkk1 is another canonical Wnt antagonist (Baron, Kneissel 2013; Gori, Baron 2013).In a rat study, it has been found that systemic treatment with Sost antibodies and Dkk1 antibodies after tooth extraction resulted in a significantly higher bone volume fraction compared to control group (Liu, Kurimoto, Zhang et al. 2018). Moreover, systemically administered Sost antibodies resulted in improved bone regeneration in large alveolar bone defects (Yao, Kauffmann, Maekawa et al. 2020).That explains the importance of canonical Wnt signaling in alveolar bone healing. In the present study, *Sfrp4* deletion did not show a significant change in socket bone healing. One possibility is that, in *Sfrp4* deletion, canonical Wnt activation and enhanced bone formation is balanced by non-canonical Wnt activation and enhanced bone resorption which in turn results in similar socket bone healing to *WT* group.

4.4 Maxillary incisor as a model for alveolar bone response study

Healing of tooth extraction socket is commonly used to study alveolar bone responses in different disease models. Molar teeth have been extensively used in mouse model because of the similarity between mice and human molars (Yuan, Pei, Zhao et al. 2018; Min, Neupane, Adhikari et al. 2019; Liu, Li, Arioka et al. 2019; Avivi-Arber, Avivi, Perez et al. 2018). Viera established the maxillary incisor alveolar socket healing model in mice and concluded that its morphological aspects of bone healing are very similar to that of alveolar bone healing previously described in other animal and human models (Vieira, Repeke, Ferreira et al. 2015). In the same study, authors found that alveolar socket of maxillary incisors are completely healed and totally filled with newly formed bone in 21 days. Our μCT findings of alveolar socket healing in *WT* and *Sfrp4 KO* groups at 3 weeks correspond with the results of *WT* mice alveolar socket healing in Viera group study at the same time point (BV/TV ≈ 60 %).

Several studies have used the maxillary incisor model in mice to investigate alveolar bone healing as this requires less manipulation of alveolar bone and produces less damage to surrounding tissues and therefore reduces the chance of introducing more confounding factors during alveolar bone healing (Colavite, Vieira, Palanch et al. 2018; Biguetti, De Oliva, Healy et al. 2019; Strauss, Stähli, Kobatake et al. 2020). Since *Sfrp4* deletion results in the same bone phenotype in both genders, we combined males and females in our analysis for *WT* and *Sfrp4 KO* groups (Kiper, Saito, Gori et al. 2016; Chen, Ng , Chen et al. 2019; Bommage, Liu, Hansen et al 2014). Comparable number of each gender were used in *WT* and *Sfrp4 KO* groups.

4.5 Clinical implications and future directions

The current study provides insights into the role of *Sfrp4* deletion and therefore of activation of canonical and non-canonical Wnt signaling cascades in alveolar bone homeostasis and bone healing after tooth extraction. Given that our previous studies (Kiper, Saito, Gori et al.

2016; Chen, Ng, Chen et al. 2019) have shown that Wnt signaling fine-tuning is critical to achieve proper bone responses and based on the findings that canonical Wnt signaling activation is associated with accelerated bone repair, this study allowed us to understand the role of non-canonical Wnt signaling (*Sfrp4* deletion) in alveolar bone responses. From a clinical point of view, our studies might have direct clinical applications for patients with Pyle's disease who presents with dental abnormalities requiring tooth extraction. To extend our understanding of role of *Sfrp4* in dentoalveolar complex, it will be interesting to investigate the effect of *Sfrp4* deletion in different dental hard tissues and evaluate its effect on dental implants osseointegration.

5 Conclusion

Similar to the phenotype seen in long bones, in alveolar bone, *Sfrp4* deletion leads to a significant decrease in cortical bone volume and increased porosity in both the incisor and molars alveolar bone areas. On the other hand, Incisor socket bone healing is not affected by *Sfrp4* deletion, suggesting that simultaneous activation of canonical and non-canonical Wnt cascades by *Sfrp4* deletion does not impair socket bone healing.

6 References

1- Gorlin RJ, Koszalka MF, Spranger J. Pyle's disease (familial metaphyseal dysplasia). A presentation of two cases and argument for its separation from craniometaphyseal dysplasia. J Bone Joint Surg Am. 1970 Mar;52(2):347-54. PMID: 5440013.

2- Raad MS, Beighton P. Autosomal recessive inheritance of metaphyseal dysplasia (Pyle disease). Clin Genet. 1978 Nov;14(5):251-6. doi: 10.1111/j.1399-0004.1978.tb02142.x. PMID: 709903.

3- Kiper POS, Saito H, Gori F, Unger S, Hesse E, Yamana K, Kiviranta R, Solban N, Liu J, Brommage R, Boduroglu K, Bonafé L, Campos-Xavier B, Dikoglu E, Eastell R, Gossiel F, Harshman K, Nishimura G, Girisha KM, Stevenson BJ, Takita H, Rivolta C, Superti-Furga A, Baron R. Cortical-Bone Fragility--Insights from sFRP4 Deficiency in Pyle's Disease. N Engl J Med. 2016 Jun 30;374(26):2553-2562. doi: 10.1056/NEJMoa1509342. PMID: 27355534; PMCID: PMC5070790.

4- Gori F, Baron R: Wnt signaling in skeletal homeostasis and diseases. Osteoporosis. edn 4. Academic Press/Elsevier; 2013:411-428:. [chapter 18].

5- Chen K, Ng PY, Chen R, Hu D, Berry S, Baron R, Gori F. Sfrp4 repression of the Ror2/Jnk cascade in osteoclasts protects cortical bone from excessive endosteal resorption. Proc Natl Acad Sci U S A. 2019 Jul 9;116(28):14138-14143. doi: 10.1073/pnas.1900881116. Epub 2019 Jun 25. PMID: 31239337; PMCID: PMC6628642.

6- Narayananan VS, Ashok L, Mamatha GP, Rajeshwari A, Prasad SS. Pyle's disease: an incidental finding in a routine dental patient. Dentomaxillofac Radiol. 2006 Jan;35(1):50-4. doi: 10.1259/dmfr/44987850. PMID: 16421266.

7- Leimeister C, Bach A, Gessler M. Developmental expression patterns of mouse sFRP genes encoding members of the secreted frizzled related protein family. Mech Dev. 1998 Jul;75(1-2):29-42. doi: 10.1016/s0925-4773(98)00072-0. PMID: 9739103.

8- Logan CY, Nusse R. The Wnt signaling pathway in development and disease. Annu Rev Cell Dev Biol. 2004;20:781-810. doi: 10.1146/annurev.cellbio.20.010403.113126. PMID: 15473860.

9- Baron R, Kneissel M. WNT signaling in bone homeostasis and disease: from human mutations to treatments. Nat Med. 2013 Feb;19(2):179-92. doi: 10.1038/nm.3074. Epub 2013 Feb 6. PMID: 23389618.

10- Tamura M, Nemoto E, Sato MM, Nakashima A, Shimauchi H. Role of the Wnt signaling pathway in bone and tooth. Front Biosci (Elite Ed). 2010 Jun 1;2:1405-13. doi: 10.2741/e201. PMID: 20515813.

11- Majidinia M, Sadeghpour A, Yousefi B. The roles of signaling pathways in bone repair and regeneration. J Cell Physiol. 2018 Apr;233(4):2937-2948. doi: 10.1002/jcp.26042. Epub 2017 Aug 3. PMID: 28590066.

12- Pyle, E. "A case of unusual bone development." *JBJS.* 1931;13(4):874-876.

13- Heselson NG, Raad MS, Hamersma H, Cremin BJ, Beighton P. The radiological manifestations of metaphyseal dysplasia (Pyle disease). Br J Radiol. 1979 Jun;52(618):431-40. doi: 10.1259/0007-1285-52-618-431. PMID: 465917.

14- Beighton P. Pyle disease (metaphyseal dysplasia). J Med Genet. 1987 Jun;24(6):321-4. doi: 10.1136/jmg.24.6.321. PMID: 3612703; PMCID: PMC1050096.

15- Styrkarsdottir U, Halldorsson BV, Gretarsdottir S, Gudbjartsson DF, Walters GB, Ingvarsson T, Jonsdottir T, Saemundsdottir J, Center JR, Nguyen TV, Bagger Y, Gulcher JR, Eisman JA, Christiansen C, Sigurdsson G, Kong A, Thorsteinsdottir U, Stefansson K. Multiple genetic loci for bone mineral density and fractures. N Engl J Med. 2008 May 29;358(22):2355-65. doi: 10.1056/NEJMoa0801197. Epub 2008 Apr 29. PMID: 18445777.

16- Cho YS, Go MJ, Kim YJ, Heo JY, Oh JH, Ban HJ, Yoon D, Lee MH, Kim DJ, Park M, Cha SH, Kim JW, Han BG, Min H, Ahn Y, Park MS, Han HR, Jang HY, Cho EY, Lee JE, Cho NH, Shin C, Park T, Park JW, Lee JK, Cardon L, Clarke G, McCarthy MI, Lee JY, Lee JK, Oh B, Kim HL. A large-scale genome-wide association study of Asian populations uncovers genetic factors influencing eight quantitative traits. Nat Genet. 2009 May;41(5):527-34. doi: 10.1038/ng.357. Epub 2009 Apr 26. PMID: 19396169.

17- Yin X, Li J, Salmon B, Huang L, Lim WH, Liu B, Hunter DJ, Ransom RC, Singh G, Gillette M, Zou S, Helms JA. Wnt Signaling and Its Contribution to Craniofacial Tissue Homeostasis. J Dent Res. 2015 Nov;94(11):1487-94. doi: 10.1177/0022034515599772. Epub 2015 Aug 18. PMID: 26285808.

18- Lim WH, Liu B, Mah SJ, Yin X, Helms JA. Alveolar bone turnover and periodontal ligament width are controlled by Wnt. J Periodontol. 2015 Feb;86(2):319-26. doi: 10.1902/jop.2014.140286. Epub 2014 Oct 27. PMID: 25345341.

19- Li J, Yin X, Huang L, Mouraret S, Brunski JB, Cordova L, Salmon B, Helms JA. Relationships among Bone Quality, Implant Osseointegration, and Wnt Signaling. J Dent Res. 2017 Jul;96(7):822-831. doi: 10.1177/0022034517700131. Epub 2017 Mar 22. PMID: 28571512; PMCID: PMC5480808.

20- Araújo MG, Silva CO, Misawa M, Sukekava F. Alveolar socket healing: what can we learn? Periodontol 2000. 2015 Jun;68(1):122-34. doi: 10.1111/prd.12082. PMID: 25867983.

21- Chappuis V, Araújo MG, Buser D. Clinical relevance of dimensional bone and soft tissue alterations post-extraction in esthetic sites. Periodontol 2000. 2017 Feb;73(1):73-83. doi: 10.1111/prd.12167. PMID: 28000281.

22- Avivi-Arber L, Avivi D, Perez M, Arber N, Shapira S. Impaired bone healing at tooth extraction sites in CD24-deficient mice: A pilot study. PLoS One. 2018 Feb

1;13(2):e0191665. doi: 10.1371/journal.pone.0191665. PMID: 29390019; PMCID: PMC5794094.

23- Jiang F, Yang X, Meng X, Zhou Z, Chen N. Effect of CBX7 deficiency on the socket healing after tooth extractions. J Bone Miner Metab. 2019 Jul;37(4):584-593. doi: 10.1007/s00774-018-0958-4. Epub 2018 Sep 20. PMID: 30238429.

24- Liu Y, Li Z, Arioka M, Wang L, Bao C, Helms JA. WNT3A accelerates delayed alveolar bone repair in ovariectomized mice. Osteoporos Int. 2019 Sep;30(9):1873-1885. doi: 10.1007/s00198-019-05071-x. Epub 2019 Jul 23. PMID: 31338519; PMCID: PMC7007703.

25- Strauss FJ, Stähli A, Kobatake R, Tangl S, Heimel P, Apaza Alccayhuaman KA, Schosserer M, Hackl M, Grillari J, Gruber R. miRNA-21 deficiency impairs alveolar socket healing in mice. J Periodontol. 2020 May 12. doi: 10.1002/JPER.19-0567. Epub ahead of print. PMID: 32396233.

26- Cook, Margaret J. The Anatomy of the Laboratory Mouse. Academic Press, 1965.

27- Bouxsein ML, Boyd SK, Christiansen BA, Guldberg RE, Jepsen KJ, Müller R. Guidelines for assessment of bone microstructure in rodents using micro-computed tomography. J Bone Miner Res. 2010 Jul;25(7):1468-86. doi: 10.1002/jbmr.141. PMID: 20533309.

28- Dempster DW, Compston JE, Drezner MK, Glorieux FH, Kanis JA, Malluche H, Meunier PJ, Ott SM, Recker RR, Parfitt AM. Standardized nomenclature, symbols, and units for bone histomorphometry: a 2012 update of the report of the ASBMR Histomorphometry Nomenclature Committee. J Bone Miner Res. 2013 Jan;28(1):2-17. doi: 10.1002/jbmr.1805. PMID: 23197339; PMCID: PMC3672237.

29- Kuchler U, Schwarze UY, Dobsak T, Heimel P, Bosshardt DD, Kneissel M, Gruber R. Dental and periodontal phenotype in sclerostin knockout mice. Int J Oral Sci. 2014 Jun;6(2):70-6. doi: 10.1038/ijos.2014.12. Epub 2014 Apr 4. PMID: 24699186; PMCID: PMC5130054.

30- Zhou S, Wang G, Qiao L, Ge Q, Chen D, Xu Z, Shi D, Dai J, Qin J, Teng H, Jiang Q. Age-dependent variations of cancellous bone in response to ovariectomy in C57BL/6J mice. Exp Ther Med. 2018 Apr;15(4):3623-3632. doi: 10.3892/etm.2018.5839. Epub 2018 Feb 6. PMID: 29545892; PMCID: PMC5841068.

31- Liu M, Kurimoto P, Zhang J, Niu QT, Stolina M, Dechow PC, Feng JQ, Hesterman J, Silva MD, Ominsky MS, Richards WG, Ke H, Kostenuik PJ. Sclerostin and DKK1 Inhibition Preserves and Augments Alveolar Bone Volume and Architecture in Rats with Alveolar Bone Loss. J Dent Res. 2018 Aug;97(9):1031-1038. doi: 10.1177/0022034518766874. Epub 2018 Apr 4. PMID: 29617179.

32- Yao Y, Kauffmann F, Maekawa S, Sarment LV, Sugai JV, Schmiedeler CA, Doherty EJ, Holdsworth G, Kostenuik PJ, Giannobile WV. Sclerostin antibody stimulates periodontal

regeneration in large alveolar bone defects. Sci Rep. 2020 Oct 1;10(1):16217. doi: 10.1038/s41598-020-73026-y. PMID: 33004873; PMCID: PMC7530715.

33- Yuan X, Pei X, Zhao Y, Tulu US, Liu B, Helms JA. A Wnt-Responsive PDL Population Effectuates Extraction Socket Healing. J Dent Res. 2018 Jul;97(7):803-809. doi: 10.1177/0022034518755719. Epub 2018 Feb 8. PMID: 29420105; PMCID: PMC6728586.

34- Min KK, Neupane S, Adhikari N, Sohn WJ, An SY, Kim JY, An CH, Lee Y, Kim YG, Park JW, Lee JM, Kim JY, Suh JY. Effects of resveratrol on bone-healing capacity in the mouse tooth extraction socket. J Periodontal Res. 2020 Apr;55(2):247-257. doi: 10.1111/jre.12710. Epub 2019 Dec 3. PMID: 31797379.

35- Vieira AE, Repeke CE, Ferreira Junior Sde B, Colavite PM, Biguetti CC, Oliveira RC, Assis GF, Taga R, Trombone AP, Garlet GP. Intramembranous bone healing process subsequent to tooth extraction in mice: micro-computed tomography, histomorphometric and molecular characterization. PLoS One. 2015 May 29;10(5):e0128021. doi: 10.1371/journal.pone.0128021. PMID: 26023920; PMCID: PMC4449187.

36- Colavite PM, Vieira AE, Palanch Repeke CE, de Araujo Linhari RP, De Andrade RGCS, Borrego A, De Franco M, Trombone APF, Garlet GP. Alveolar bone healing in mice genetically selected in the maximum (AIRmax) or minimum (AIRmin) inflammatory reaction. Cytokine. 2019 Feb;114:47-60. doi: 10.1016/j.cyto.2018.11.027. Epub 2018 Dec 22. PMID: 30584949.

37- Biguetti CC, De Oliva AH, Healy K, Mahmoud RH, Custódio IDC, Constantino DH, Ervolino E, Duarte MAH, Fakhouri WD, Matsumoto MA. Medication-related osteonecrosis of the jaws after tooth extraction in senescent female mice treated with zoledronic acid: Microtomographic, histological and immunohistochemical characterization. PLoS One. 2019 Jun 14;14(6):e0214173. doi: 10.1371/journal.pone.0214173. PMID: 31199812; PMCID: PMC6568384.

38- Brommage R, Liu J, Hansen GM, Kirkpatrick LL, Potter DG, Sands AT, Zambrowicz B, Powell DR, Vogel P. High-throughput screening of mouse gene knockouts identifies established and novel skeletal phenotypes. Bone Res. 2014 Oct 28;2:14034. doi: 10.1038/boneres.2014.34. PMID: 26273529; PMCID: PMC4472125.